Supporting Information

Sun et al. 10.1073/pnas.1109546108

SI Materials and Methods

RNA Isolation, Quantitative PCR, and Real-Time PCR. Cellular RNA was prepared from skeletal muscle or C2C12 cells using TRIzol reagent (Invitrogen), and real-time PCR was performed with iQ SYBR Green Supermix using the iCycler iQ real-time PCR detection system (Bio-Rad).

Primers for the different isoforms of NADPH oxidase (Nox) were:

Nox1 forward: ACCTGCTCATTTTGCAACCGTA
Nox1 reverse: AGAGATCCATCCATGGCCTGTT
Nox2 forward: CGACAAGGATTCGAAGACAACTG
Nox2 reverse: AATACCGGTCAGAAATCCCGACT
Nox3 forward: CAGTCGGAACTTCATTTCACTGGT
Nox3 reverse: AGGTGATAACGCTCCAGGTTGAA
Nox4 forward: CATGGTGGTGGTATTGTTCCTCA
Nox4 reverse: GCCAGGAGGGTGAGTGTCTACAT
Dual oxidase (Duox) 1 forward: TATTTCGAGGGGAGTGGATTTGG
Duox1 reverse: CCCTACAAGCTTCTCCGACATGA
Duox2 forward: GTGTGCGCCTGTTACTGTGATTG
Duox2 reverse: CCATCACTGGCTGGTTGTTTCTT.

Western Blot Analysis. Samples were separated by SDS/PAGE on 4–12% gradient gels and blotted to nitrocellulose membrane. Ryanodine receptor–Ca^{2+} release channel (RyR1) and Nox4 were detected, respectively, with anti-ryanodine receptor (anti-RyR) mouse monoclonal antibody (Clone 34C; (Affinity BioReagents) and one of two anti-Nox4 polyclonal antisera (rabbit: ThermoScientific; goat: Santa Cruz).

Coimmunoprecipitation. Rabbit sarcoplasmic reticulum (SR) vesicles were solubilized in 50 mM Tris (pH 7.4), 0.9% NaCl, 10 μM Ca^{2+}, and 0.5% Triton X-100 (Sigma-Aldrich) with protease inhibitors before incubation overnight at 4 °C with mouse monoclonal anti-RyR1 antibody (as above), followed by incubation with protein G Sepharose (Amersham Biosciences) for 1 h. Following elution and Western blotting, RyR1 was detected with the immunoprecipitating antibody, and Nox4 was detected with goat polyclonal antiserum (Santa Cruz).

Immunohistochemistry. Rat hind-limb extensor muscle was sectioned at 8-μM thickness on a cryostat, and slide-mounted sections were fixed by immersion in 4% paraformaldehyde, washed, permeabilized with 0.1% Triton X-100 in PBS, and blocked with 1% goat serum in PBS. Sections then were incubated overnight with anti-Nox4 rabbit polyclonal antibody (provided by David Lambeth, Emory University, Atlanta, GA) or anti-RYR1 mouse monoclonal antibody (as above) followed by, respectively, Alexa Fluor 488-conjugated goat anti-rabbit IgG or Alexa Fluor 546-conjugated goat anti-mouse IgG (Molecular Probes) for 1 h. Stained sections were analyzed by confocal scanning-laser microscopy (Zeiss LSM510).

siRNA-Mediated Knockdown of Nox4 in C2C12 Cells. C2C12 cells were grown in DMEM (Gibco) containing 10% FBS and penicillin/streptomycin, then were transferred to Opti-MEM medium without serum (Gibco), and were transfected by electroporation with 500 nM Nox4 siRNA or scrambled control siRNA (Dharmacon). Cells were allowed to reach confluency, after which they were transferred to DMEM containing 2% horse serum for differentiation to myotubes and myofibers. Microsomal fractions were isolated from differentiated cells scraped from tissue culture plates using the same scheme of differential centrifugation as used to generate the microsomal fraction from skeletal muscle (*Materials and Methods*).

Assay of Intracellular Ca^{2+} Release: C2C12 Cells. C2C12 cells were grown on coverslips (40-mm diameter) and allowed to differentiate for 9 d after siRNA transfection. Myotubes then were loaded for 30 min with the Ca^{2+} indicators Fluo 3-AM (5 μM) and Fura Red (10 μM) in DMEM and 0.06% pluronic acid F127. For measurement at controlled partial pressure of O_2 (pO_2), coverslips were placed in a closed, live-cell imaging chamber under a continuous flow of DMEM/50 mM Tris-HCl (pH 7.4) that was preadjusted with O_2 (1% or 20%), 5% CO_2, remainder N_2 to the specified pO_2 (10 mm Hg or 150 mm Hg). Ca^{2+} release was induced by depolarization with 50 mM KCl (final concentration) in DMEM. Ca^{2+}-induced fluorescence was imaged with a confocal scanning-laser microscope (Zeiss LSM510), and signal strength was quantified as F1 (peak Fluo 3 signal)/F0 (baseline Fluo 3 signal). Fura Red fluorescence was monitored to confirm the Ca^{2+} dependence of Fluo 3 signals.

Construction and Administration of Nox4 shRNA–Adeno-Associated Virus Vector. Origene plasmids (pRS series) containing the U6 promoter sequence and one of two shRNAs targeting mouse Nox4 (sequence A: ATCCAGCTGTACCTCAGTCAAACAGATCG; sequence B: AACACCTCTGCCTGCTCATTTGGCTGTCC) or a scrambled negative control (GCACTACCAGAGCTAACTCAGATAGTACT) were obtained and validated for knockdown of Nox4. The neomycin gene present in the pTRUFr plasmid (1) was removed via BstBI and BclI digestion and blunt-ended. The blunted EcoRI/SalI fragment (containing the U6 promoter-shRNA cassette) from each Origene plasmid was used to replace the neomycin gene in pTRUFr. The resulting adeno-associated virus (AAV) plasmids contained the Nox4 shRNA expression cassette as well as a CMV-GFP cassette. The integrity of the U6-shRNA cassette was confirmed by HindIII digestion as well as by DNA sequencing. Recombinant AAV serotype 6 (rAAV6) Nox4 shRNA vectors were produced using procedures as reviewed (2). Briefly, HEK-293 cells were cotransfected with plasmids encoding AAV rep-cap (pXR-6), adenovirus helper XX6-80, and individual AAV Nox4 shRNA plasmids. Cells were harvested 48–72 h posttransfection and were lysed by freeze-thawing. rAAV was isolated by two sequential cesium gradient centrifugations. Each fraction was monitored following gradient centrifugation by dot blot or by infecting HeLa cells and then by assessing GFP expression with fluorescence microscopy. AAV then was concentrated and titered by dot blot. For each mouse, the left and right hind-limbs were injected with 1.3×10^{11} viral particles containing either Nox4 or control scrambled shRNA. Injections were percutaneous and targeted the gastrocnemius muscle using a 28-gauge needle and 50-μL injection volume. After 4 wk (a survival interval determined by examining the time-course of knockdown in preliminary experiments), extensor digitorum longus (EDL) muscles were removed for bioassay, and the extent of Nox4 knockdown in each muscle was assessed by Western blotting for Nox4 after bioassay. In addition, GFP expression and RyR1 protein level also were assessed by Western blotting. Muscles without detectable GFP expression or exhibiting more than twofold increased RyR1 expression ($n = 2$) were excluded from analysis.

Data Analysis. Data were analyzed with one-way or two-way ANOVA with an appropriate post hoc test for comparison of multiple groups or unpaired student's *t* test for comparison between two groups.

1. Haberman RP, McCown TJ, Samulski RJ (1998) Inducible long-term gene expression in brain with adeno-associated virus gene transfer. *Gene Ther* 5:1604–1611.
2. Grieger JC, Choi VW, Samulski RJ (2006) Production and characterization of adeno-associated viral vectors. *Nat Protoc* 1:1412–1428.

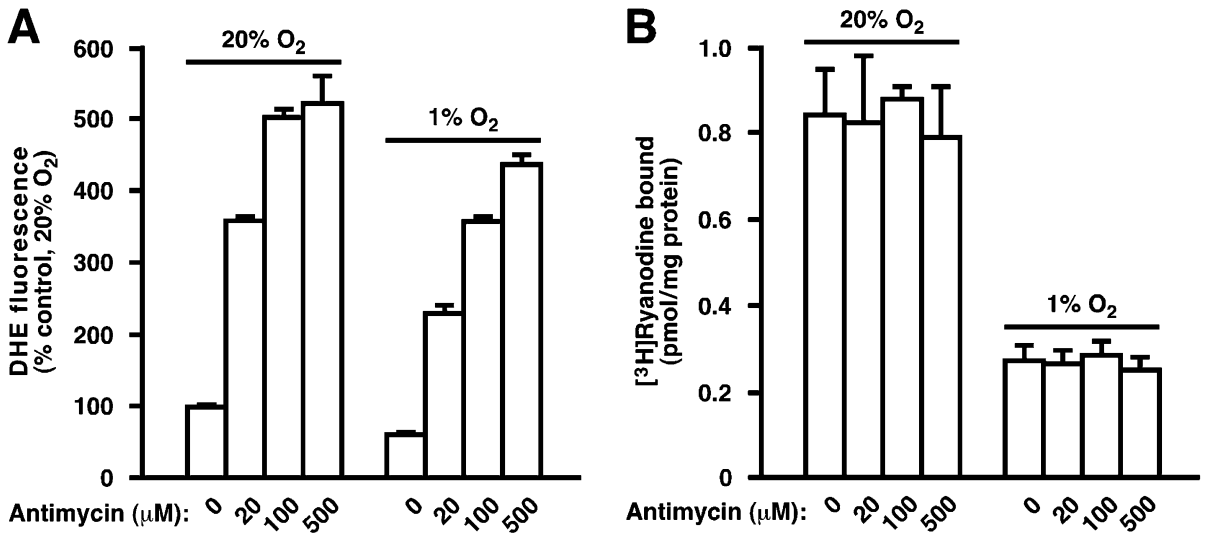

Fig. S1. A subpopulation of mitochondria is intimately associated with the SR (1). (*A*) ROS production by mitochondria is increased in the presence of the uncoupling agent antimycin A (2), and exposure to antimycin A resulted in dose-dependent increases in ROS production by SR vesicles at both high and low pO_2 as assessed by dihydroethidium (DHE) fluorescence. (*B*) Strikingly, however, no change in RyR1 activity was associated with antimycin A treatment as assessed by [^{3}H]-ryanodine binding (n = 4–6).

1. Rossi D, Barone V, Giacomello E, Cusimano V, Sorrentino V (2008) The sarcoplasmic reticulum: An organized patchwork of specialized domains. *Traffic* 9:1044–1049.
2. Chen Q, Vazquez EJ, Moghaddas S, Hoppel CL, Lesnefsky EJ (2003) Production of reactive oxygen species by mitochondria: Central role of complex III. *J Biol Chem* 278:36027–36031.

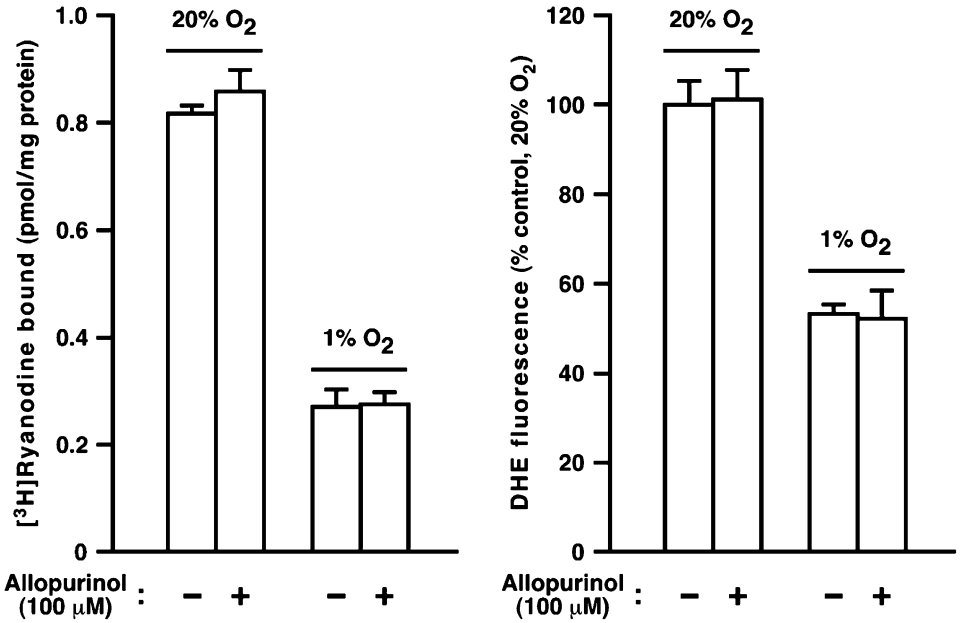

Fig. S2. In SR vesicles isolated from rabbit hind-limb muscle, incubation with the xanthine oxidase inhibitor allopurinol had no effect on the activity of the ryanodine receptor/Ca^{2+} channel as assessed by [^{3}H]ryanodine binding (*Left*) or on production of reactive oxygen species (ROS) as assessed by DHE-derived fluorescence (*Right*), at either low pO_2 (1% O_2) or high pO_2 (20% O_2).

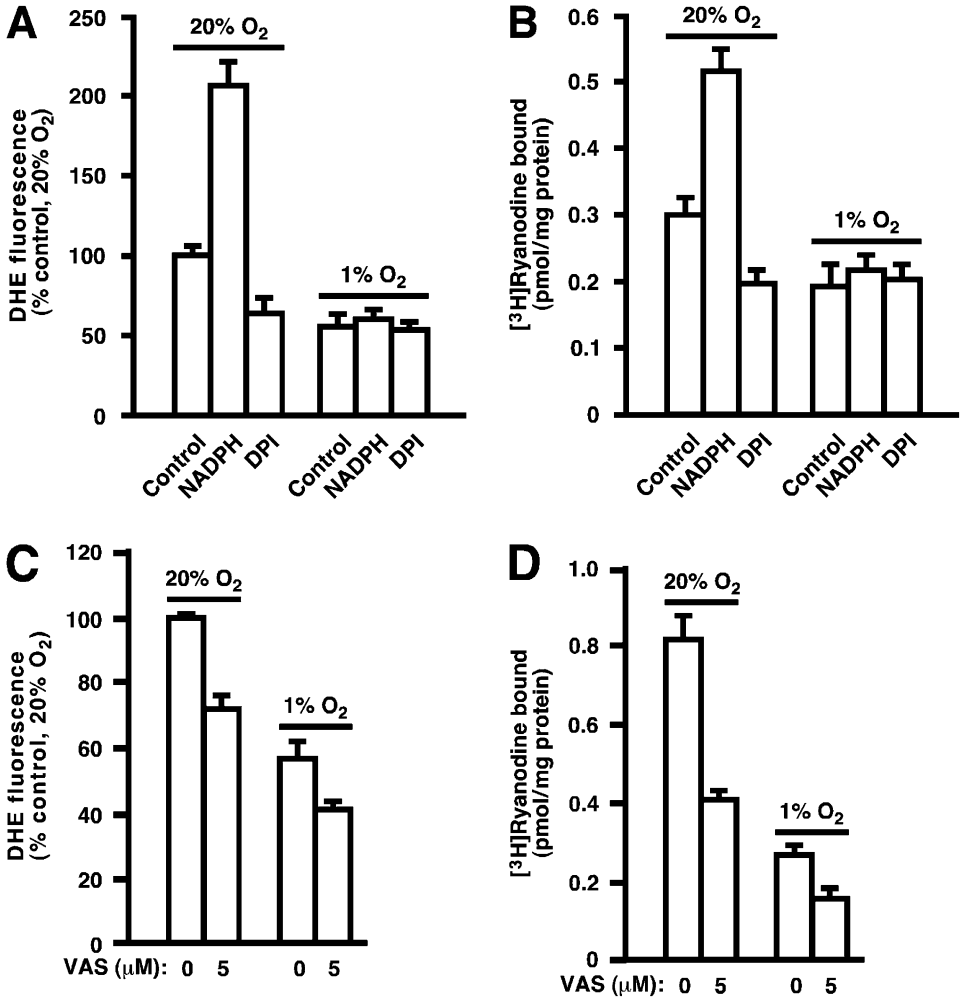

Fig. S3. (*A* and *B*) In SR vesicles isolated from skeletal muscle of mouse, ROS production (*A*) and RyR1 activity (*B*) were enhanced at high versus low pO_2. At high pO_2 but not at low pO_2, the addition of NADPH (1 mM) enhances production of ROS, and this enhancement is eliminated by DPI. (*C* and *D*) In SR vesicles isolated from skeletal muscle of rabbit, the Nox inhibitor 3-benzyl-7-(benzoxazolyl)thio-1,2,3-triazolo[4,5-d]pyrimidine (VAS2870, VAS) also suppressed ROS production (*C*) and RyR activity (*D*) at both high and low pO_2. *A*–*D*: n = 4–6.

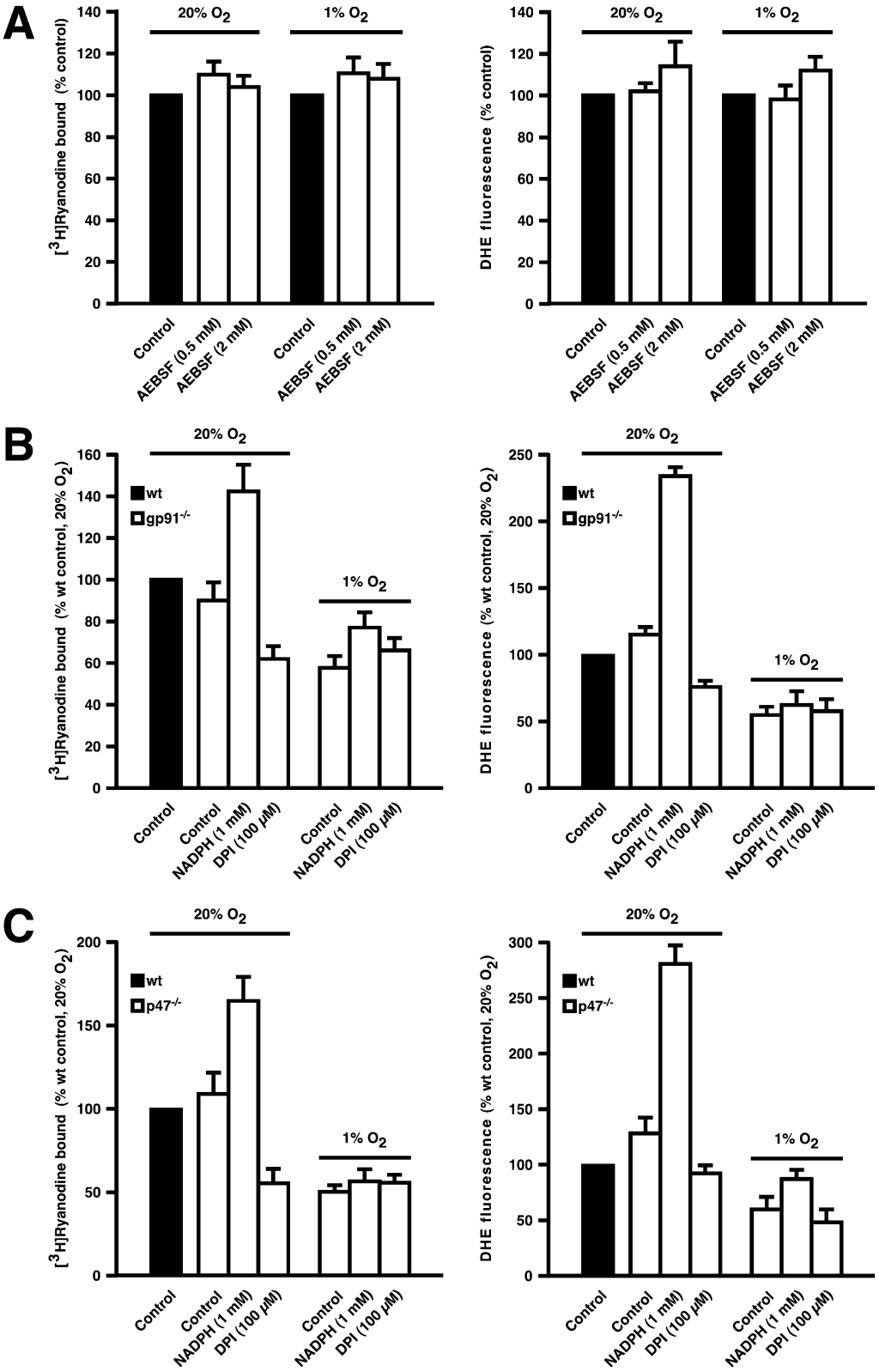

Fig. S4. (*A*) In SR vesicles isolated from skeletal muscle of rabbit, the Nox2 inhibitor aminoethyl-benzenesulfono-fluoride (AEBSF) had no effect on RyR activity ([^{3}H]-ryanodine binding) or ROS production (DHE fluorescence) (n = 3). (*B* and *C*) The effects of pO_2 on ROS production (*Left*) and on RyR activity (*Right*) were indistinguishable in SR vesicles prepared from hind-limb muscle of wild-type (Fig. 2), $gp9^{-/-}$ knockout mice (*B*) or $p47^{-/-}$ knockout mice (*C*) (n = 3 for all conditions). $Gp91^{phox}$ is an essential component of the flavocytochrome core of Nox2, and $p47^{phox}$ is an obligate cytosolic component of Nox2 (1). Note that ROS production and RyR1 activity were enhanced by NADPH in SR vesicles derived from these Nox2-mutant mice, and pO_2-dependent enhancement of O_2^- production and RyR1 activity was eliminated by DPI, indicating the operation of an alternative Nox. Therefore, it is unlikely that Nox2 serves as a pO_2-dependent source of ROS in the isolated SR.

1. Bedard K, Krause KH (2007) The NOX family of ROS-generating NADPH oxidases: Physiology and pathophysiology. *Physiol Rev* 87:245–313.

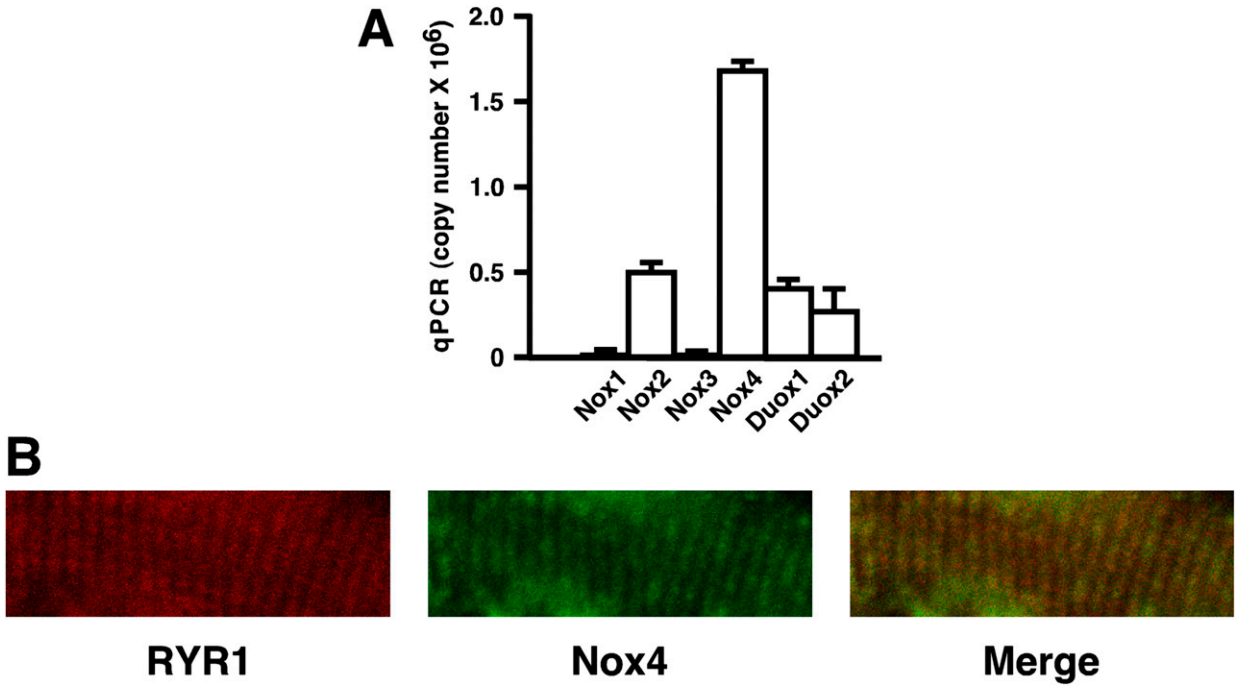

Fig. S5. Expression of Nox4 in skeletal muscle and colocalization with RyR1. (*A*) Quantitative real-time PCR (qPCR) indicated that Nox2 and Nox4 as well as Duox1 and Duox2 are expressed at significant levels in rat hind-limb skeletal muscle and that Nox4 is the most abundant species (n = 3). (*B*) Confocal microscopic imaging of a representative section of rat hind-limb extensor muscle stained immunohistochemically for RyR1 (red) and for Nox4 (green) indicates essentially complete colocalization of Nox4 with RyR1, whereas a portion of RyR1 does not colocalize with Nox4.

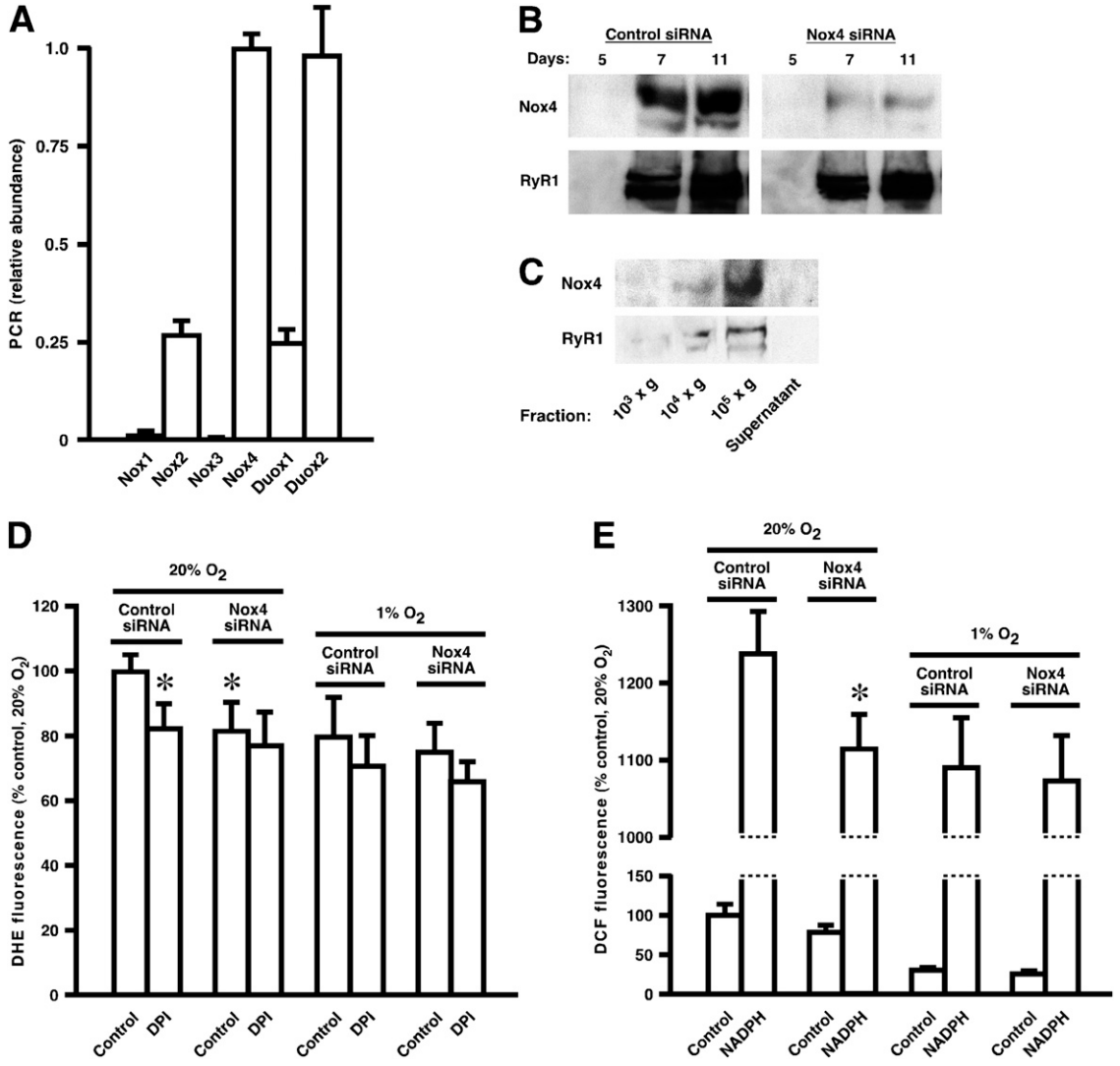

Fig. S6. ROS generated by Nox4 mediate pO_2-dependent regulation of RyR1 in C2C12 cells. (*A*) In differentiated C2C12 cells, Nox4 is relatively abundant as assessed by PCR. (*B*) A representative Western blot illustrates coexpression of Nox4 and RyR as C2C12 cells differentiate in culture and near-total suppression of Nox4 expression by treatment with a Nox4-specific siRNA (with no effect on RyR expression). Note that C2C12 cells express RyR3 as well as RyR1 (1) and that RyR3, which has a higher gel mobility than RyR1 (2), also is detected by the antibody used. (*C*) Subcellular fractionation of differentiated C2C12 cells shows that Nox4 and RyR1 are most abundant in the microsomal (100,000 × *g*) fraction. (*D*) Production of ROS by the microsomal fraction (assessed by DHE fluorescence) was enhanced at high versus low pO_2, and this enhancement was abrogated by DPI (20 μM) and by siRNA-mediated knockdown of Nox4 ($n = 4$). (*E*) Production of H_2O_2 by the microsomal fraction [assessed by 2′,7′-dichlorofluorescein (DCF) fluorescence] is enhanced at high versus low pO_2 and by the addition of NADPH (1 mM), and enhancement is abrogated by siRNA-mediated knockdown of Nox4 ($n = 4$). *$P < 0.05$ versus control siRNA at 20% O_2.

1. Wang Y, et al. (2006) Knocking down type 2 but not type 1 calsequestrin reduces calcium sequestration and release in C2C12 skeletal muscle myotubes. *J Biol Chem* 281:15572–15581.
2. Murayama T, Ogawa Y (1997) Characterization of type 3 ryanodine receptor (RyR3) of sarcoplasmic reticulum from rabbit skeletal muscles. *J Biol Chem* 272:24030–24037.

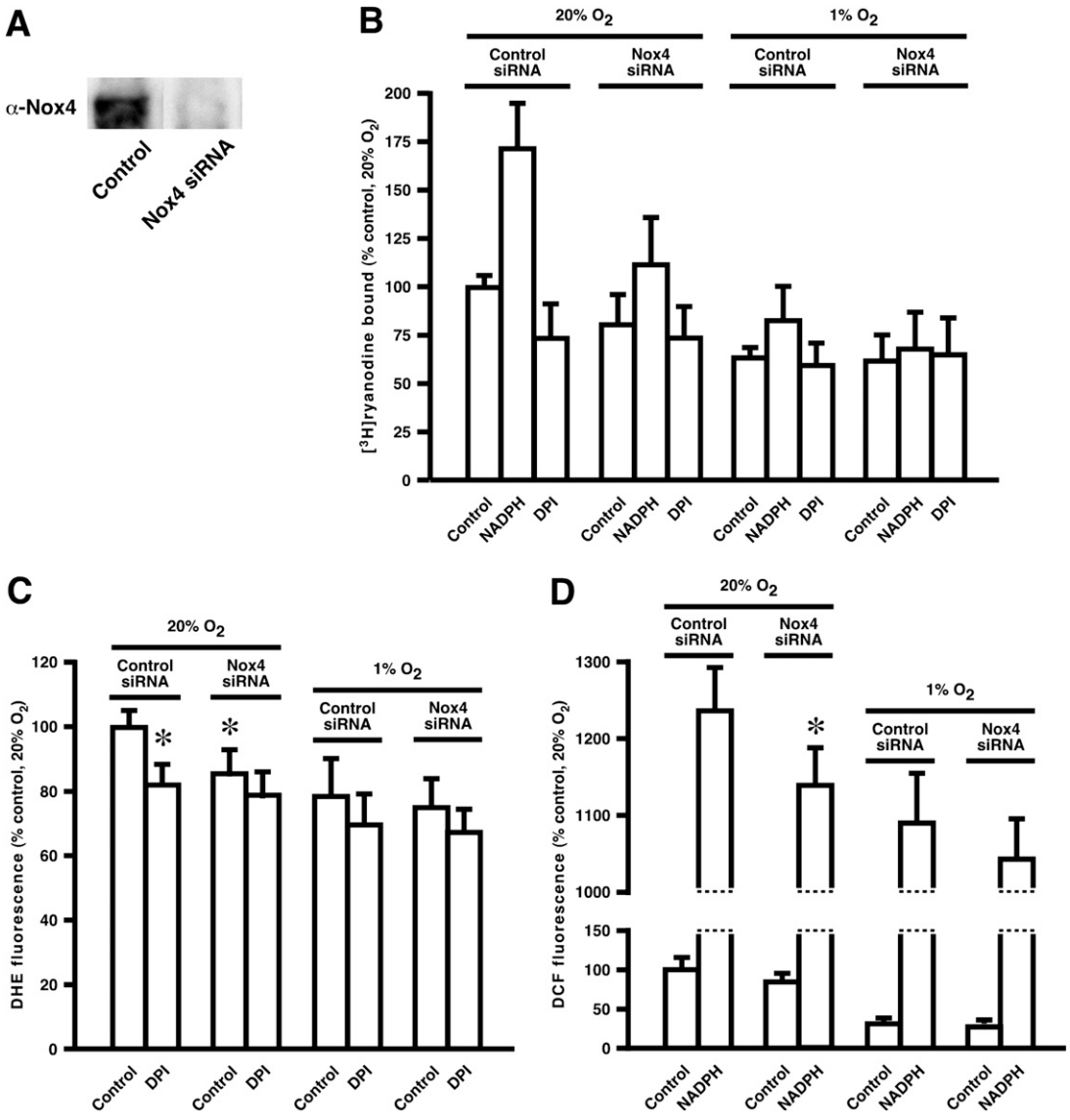

Fig. S7. Use of a second, nonoverlapping siRNA verified that knockdown of Nox 4 in C2C12 cells (*A*) eliminated the effects of pO_2 on RyR1 activity (*B*) and ROS production (*C* and *D*). *$P < 0.05$ versus control at 20% O_2; $n = 4$ for all conditions.

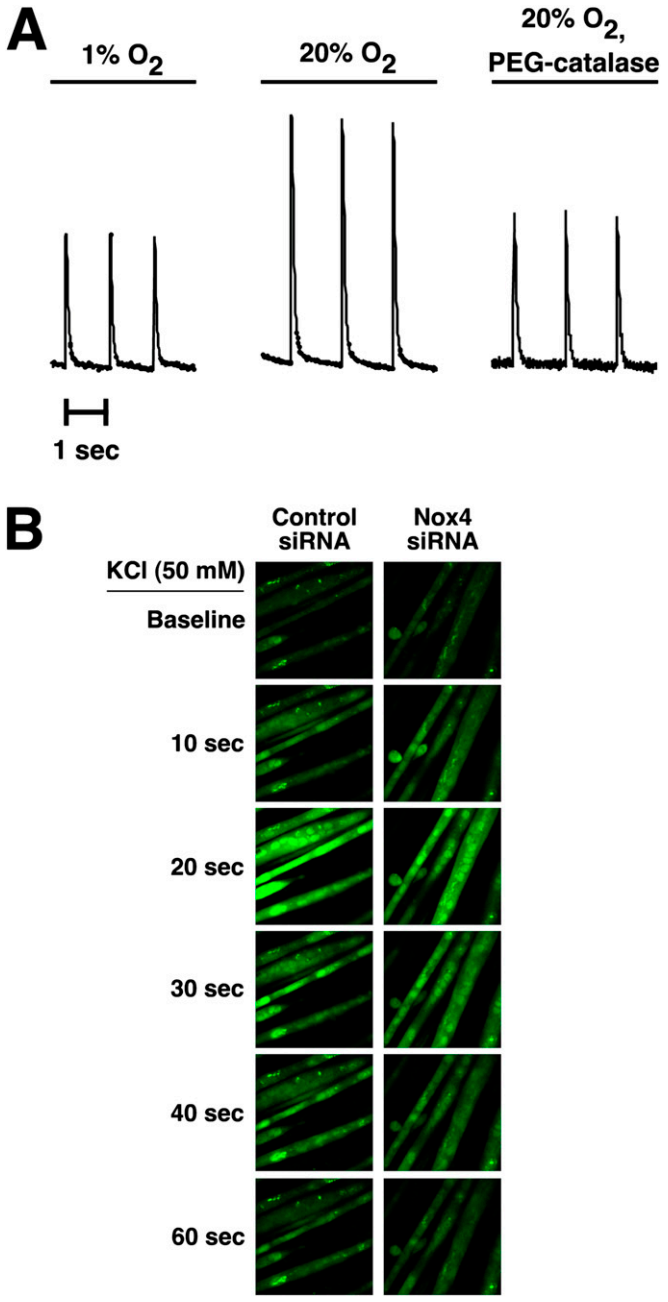

Fig. S8. (*A*) Examples of electrically induced Ca^{2+} transients in primary myocytes (flexor digitorum brevis) derived (F/F_o) from Fluo 3-AM fluorescence. (*B*) Two exemplary time series of Fluo 3-AM fluorescence (imaged by laser-scanning confocal microscopy; four or five myofibers are visible in each series) following K^+-induced depolarization of C2C12 cells treated with control or Nox4-specific siRNA. Peg-catalase, polyethylene glycol catalase.

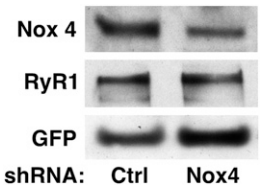

Fig. S9. Western blots illustrating knockdown of Nox4 (without effects on RyR1) in a mouse EDL muscle following local administration of an AAV vector encoding shRNA. The vector used also coded for GFP, to verify infection. Control (Ctrl), infection with AAV vector encoding scrambled shRNA, injected into the opposite EDL.